



STUDY ON MICROSTRUCTURE AND CORROSION RESISTANCE OF LASER CLADDING FE BASED ALLOY COATING

Qiu Yuwei, Song dekun, Liu Lihong
School of Mechanical Engineering
Anhui University of Science and Technology
Huainan, Anhui, China

Zhang Jian, Liu jing, Li Yongfeng
Binzhou Key Laboratory of Aeronautical Structural Parts
Surface Engineering
Binzhou University
Binzhou, Shandong, Chinaline

Abstract: In order to improve the corrosion resistance of 45 steel surface, Fe-based alloy coating was prepared on the surface of 45 steel by laser cladding technology and the microstructure of Fe-based alloy coating was observed. Corrosion resistance test of Fe-based alloy coating and 45 steel in 3.5wt.% NaCl solution and 1mol/L HCl solution. The results show that the coating structure of the laser cladding Fe-based alloy is uniformly dense, and there are no obvious cracks, porosity and other defects on the surface of the coating. The self-corrosion potential (E_{corr}) of the coating and 45 steel in 3.5wt.% NaCl solution was -570.96mV and -831.15mV, and the self-corrosion current density (i_{corr}) was $12.13\mu A \cdot cm^{-2}$ and $13.70\mu A \cdot cm^{-2}$, respectively. The E_{corr} of the coating and 45 steel in the 1mol/L HCl solution were -453.45mV and -497.00mV, respectively, and the i_{corr} of the coating and 45 steel was $297.78\mu A \cdot cm^{-2}$ and $379.31\mu A \cdot cm^{-2}$, respectively. The coating has a greater arc capacitive than 45 steel, has a larger impedance modulus, and has better corrosion resistance.

Keywords: laser cladding; Fe-based alloy coating; microstructure; corrosion resistance

I. INTRODUCTION

45 steel is widely used in actual industrial production, but often the working environment of parts is very harsh, so parts are required to have good corrosion resistance. 45 steel itself does not have good corrosion resistance, but if the part itself adopts an alloy material with good corrosion resistance, it will cause unnecessary waste of resources and cannot take into account other properties of the part^[1].

The surface modification technology of the material can prepare coatings with excellent corrosion resistance on the surface of the parts, the main methods include: electroplating method, thermal spraying method, laser cladding method, electrode welding method, plasma spraying method and hardened alloy method^[2-4]. Compared with other surface modification methods, the laser cladding method has a small heating area of the workpiece during the cladding process, the workpiece is not easy to deform, and the substrate microstructure performance changes are small. Laser cladding requires less cladding material, which can precisely control the cladding range and reduce the amount of subsequent machining. The cladding layer prepared by laser cladding technology has fine grains, uniform and dense tissue, good adhesion to the coating and matrix, and easy surface processing^[5-6].

Liu^[7] studied the corrosion resistance of laser cladding Fe-based alloy coatings on the surface of 27SiMn steel, and analyzed the microstructure and corrosion resistance of cladding layers. The study found that Fe-based alloy coatings are mainly composed of α -Fe, M7C3, M2B and Cr3Si. The E_{corr} of the cladding layer is higher than that of the matrix, and the arc-tolerant radius of the cladding layer is greater than the arc-tolerant radius of the matrix. After the corrosion test, the corrosion loss of the cladding layer and the matrix was

0.0688 and 0.0993 g·cm⁻², respectively, and the corrosion loss of the cladding layer was 30.7% less than that of the matrix. A Riquelme et al^[8] used laser cladding technology to prepare SiC particle-reinforced aluminum matrix composites on the surface of AA6082 aluminum alloy. Through electrochemical corrosion experiments, the corrosion behavior of the coating in 3.5 wt.% NaCl solution was observed, and the corrosion products of the known cladding layer were Al(OH)₃ and Al₂O₃, and the corrosion products formed a film that limited the corrosion continuity, but the discontinuity of the film reduced the corrosion resistance of the coating. Zhou et al^[9] prepared an amorphous FeSiB composite coating on S355 structural steel, and studied the surface morphology, microstructure element distribution, phase composition of the coating, and used the electrochemical workstation to test the electrochemical corrosion behavior of the FeSiB coating in 3.5wt.% NaCl solution. The results show that the corrosion potential of FeSiB coating and matrix is -0.718 and -1.042V, respectively, indicating that the corrosion potential of FeSiB coating is positively displaced, and its corrosion resistance is higher than that of the matrix.

At present, many scholars have studied the microstructure and mechanical properties of Fe-based alloy coatings^[10-13], but there are fewer studies on the corrosion resistance of Fe-based alloy coatings in acid solutions and salt solutions. In view of this, this paper explores the best process parameters in combination with uniform design, prepares cladding layers with good surface quality, and studies the corrosion resistance of cladding layers, so as to accumulate experience for subsequent industrial applications.

II. EXPERIMENTEL MATERIAL AND PROTOCOL

A. Experimental equipment

The LATEC-LOM-3000 laser cladding system is shown in Figure 1: The laser nozzle is connected to the ABB robot, and the optical lens inside the laser head plays an important role in the light separation and focusing of the laser beam. The powder feeder is directly connected to the laser nozzle, which can realize the synchronous output of light and powder, in order to prevent the powder from sticking to the laser head due to high temperature, blocking the powder outlet, so the laser head is connected to the water cooler hose to ensure that the temperature of the laser head is stable. In order to prevent the specimen from reacting with elements such as O and H in the air during cladding, the Ar cylinder is connected at the laser head. The schematic diagram of laser cladding synchronous powder feeding is shown in Figure 2.



Figure 1 Laser cladding system diagram

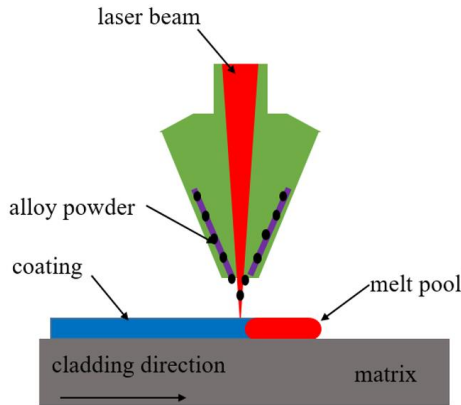


Fig. 2 Schematic diagram of laser cladding process

B. Experimental material

The main chemical composition of the laser cladding experiment is C 0.42~0.50, Cr ≤0.25, Mn 0.50~0.80, Ni≤0.25, P≤0.035, S ≤0.17~0.37, and the specifications are 200mm×100mm×10mm. Before melting, the surface of 45 steel is sanded by sandpaper, the oil and oxide scale on the surface of the substrate are removed, and scrubbed with absolute ethanol, placed in a drying box to dry, preheated and prepared, and preheated at a temperature of 200 °C. The cladding material is a new Fe-based alloy powder, and the main components are shown in Table 1.

Table 1 chemical composition of Fe based alloy powder (wt.%)

Element	B	C	Si	Cr	Co	Ni	Cu	Fe
Wt. %	0.8	0.2	0.64	15	1.75	3.25	0.21	Bal.

C. Uniformly design the experimental table

Explore excellent process parameters using a uniform design approach to prepare high-quality, high-performance cladding layers. The optimization operation is generated by the uniform design software U \times (9 \times 9 \times 3 \times 3) as shown in Table 2.

Table 2 Mixing levels of U \times (9 \times 6 \times 6 \times 3) Uniform design table

No.	Laser	scanning	Distribution	Spot
-----	-------	----------	--------------	------

	power/W	speed/(mm/s)	rate/(g/min)	diameter/(mm)
1	600	12.5	10	1.8
2	1200	12	11	2.2
3	1350	13.5	9	1.8
4	1650	13	10	2.2
5	1800	11.5	9	2
6	900	14	11	2
7	1500	10.5	11	1.8
8	1050	10	10	2
9	750	11	9	2.2

D. Preparation of coatings and specimens

In this study, the cladding layer was prepared using the LATEC-LOM-3000 laser cladding system, and different parameter combinations were obtained according to the uniform design for laser cladding. After the observation of the surface quality, dilution rate and microstructure of the coating under different process parameters in the early stage, the optimal process parameters were determined to be laser power 1050 W, scanning speed 10 mm/s, powder delivery 10 g/min, spot diameter 2 mm, defocusing amount 13.8 mm, lap rate 40%, the single-channel and multi-channel lap Fe-based alloy coating specimens clad under the process parameters were cut by EDM wire cutting machine tools, and the cutting direction was perpendicular to the cladding direction. The cut sample is thoroughly cleaned in an ultrasonic cleaner and then quickly dried to prevent rust from appearing on the surface of the substrate. Wires are wrapped with copper foil, and then the samples are cold-mounted for subsequent electrochemical corrosion tests.

E. Coating microstructure characterization and corrosion resistance test

After the laser cladding experiment, the staining layer is colored and infiltrated by using flaw detection reagents to detect whether there are macroscopic cracks and other defects on the surface of the cladding layer. Metallographic microscopy and FEI Nova Nano SEM 450 scanning electron microscope (SEM) were used to observe the microstructure morphology and composition of the cladding layer, and the corrosion resistance of the cladding layer was analyzed. The experiment uses the classic three-electrode method to study its corrosion resistance, and the experimental schematic diagram is shown in Figure 3. Use a cladding specimen or a 45 steel specimen as the working electrode (WE), and the specimen area is 1 cm². The saturated calomel electrode (SCE) is used as the reference electrode and the platinum electrode (CE) is the auxiliary electrode. The experimental medium was 3.5wt.% NaCl and 1mol/L HCl solution.

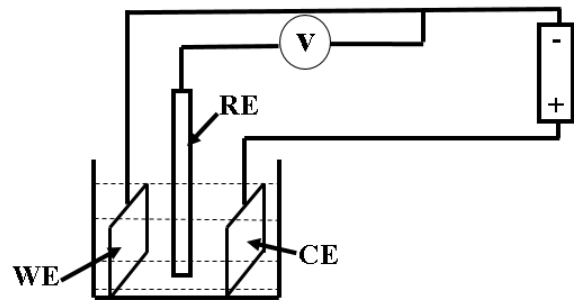


Figure 3 Schematic diagram of the three-electrode operation

III. RESULTS AND DISCUSSION

A. Macroscopic topography analysis

According to the uniform design experiment, the fe-based

alloy coating was prepared, and the macroscopic morphology of the cladding layer was shown in Figures 4(a) and 4(b). After observation, the surface of the coating shows a metallic luster, and there is no obvious crack and oxidation, and the surface of the multi-channel lap cladding layer is flat, and there is no obvious condensation ripple of the molten pool. Figures 4(c) and 4(d) are non-destructive flaw detection results of single-channel and multi-channel Fe-based alloy coatings, which show that the coating has no macroscopic cracks and the surface quality of the Fe-based alloy cladding layer is good.

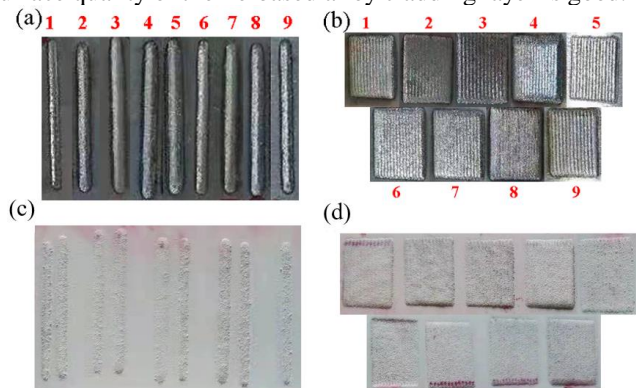


Figure 4 Macroscopic morphology of the cladding layer of laser cladding Fe-based alloy. (a) single-channel; (b) multi-channel; (c) single-channel flaw detection morphology; (d) multi-channel flaw detection morphology

B. Microstructure analysis

Fig. 5 shows the microstructure diagram of each region of the Fe-based alloy coating, which shows that the metallurgical binding between the coating and the substrate is better. As can be seen from FIG. 5 (a), near the interface of the coating, a tissue composed of planar crystals is formed. Alloy coatings prepared by laser cladding technology have different solidification rates due to large differences in temperature gradients in different parts, which in turn affects the morphology of different regions. Fig. 5(b) shows the microstructure at the bottom of the coating, where the temperature gradient decreases and a coarser columnar dendrite is precipitated. As solidification continues, the growth of the tissue in the middle of the coating gradually loses its directionality, as shown in Figure 5(c). Due to the diversification of heat dissipation methods in the top tissue of the coating, the isometric crystals with smaller grains continue to precipitate, and the microstructure is fine and uniform, as shown in Figure 5(d).

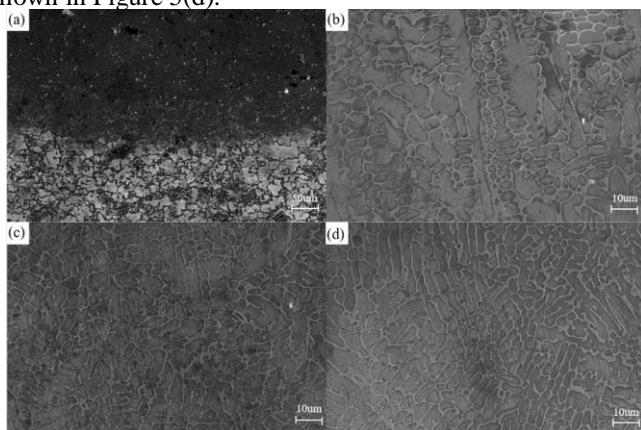


Fig. 5 Microstructure morphology of the laser cladding layer. (a) cladding boundary; (b) the bottom of the cladding layer; (c) the middle of the cladding layer; (d) the top of the cladding layer

C. Corrosion resistance analysis of cladding layer

In order to test the electrochemical corrosion properties of the 45 steel matrix and cladding layer, it was placed into a

3.5wt.% NaCl and 1mol/L HCl solution, and the polarization curve measured at room temperature is shown in Figure 6. The size of the electrochemical corrosion voltage E_{corr} to measure the corrosion tendency of the metal, the larger the value means that the corrosion tendency of the material is relatively small, the size of the electrochemical corrosion current i_{corr} to indicate the corrosion rate of the material, the larger the value the faster the corrosion rate.

The self-corrosion potential E_{corr} and self-corrosion current density i_{corr} of different materials in NaCl solution were determined by tafer curve extrapolation, and the results are shown in Table 3. The corrosion potential of the cladding layer is 261.29mV higher than that of the 45 steel matrix. The current density of the cladding layer is $12.13\mu A \cdot cm^{-2}$, which is $1.57\mu A \cdot cm^{-2}$ lower than the corrosion current density of the 45 steel matrix, so it can be shown that the corrosion rate of the cladding layer is lower than the corrosion rate of the substrate. This shows that the cladding layer inhibits the corrosion tendency of 45 steel substrates in NaCl solution to a certain extent, and reduces the corrosion rate of the substrate.

Using the same test method as the above test to detect the self-corrosion potential and self-corrosion current of cladding layer and 45 steel in HCl solution, Figure 7 is the polarization curve of three materials in HCl solution, the detection results are shown in Table 4, it can be seen that the corrosion potential of the cladding layer is -453.45mV, which is 43.55mV higher than the corrosion potential of the 45 steel substrate, so the corrosion tendency of the cladding layer is significantly lower than that of the 45 steel matrix. The corrosion current density of the cladding layer is $297.78\mu A \cdot cm^{-2}$, which is $81.53\mu A \cdot cm^{-2}$ lower than the corrosion current density of the 45 steel matrix, which shows that the corrosion rate of the cladding layer is lower than the corrosion rate of the 45 steel substrate. It can be seen that the corrosion tendency and corrosion rate of the cladding layer in the acidic solution are lower than those of the 45 steel matrix, which can better protect the 45 steel matrix from corrosion in the acidic environment.

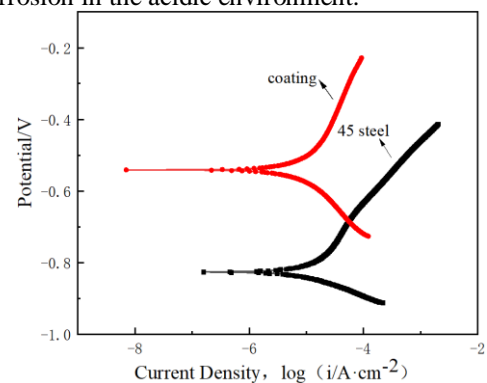


Fig. 6 Polarization curve of different materials in 3.5wt.% NaCl solution
Table 3 Electrochemical parameters of different materials in 3.5wt.% NaCl solution

Samples	Self-corrosion potential, E_{corr}/mV	Self-corrosion current density, $i_{corr}/\mu A \cdot cm^{-2}$
45 steel	-831.15	13.70
Coating	-570.96	12.13

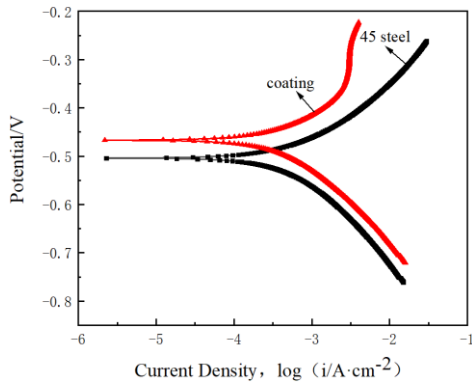


Fig. 7 Polarization curve of different materials in 1mol/L HCl solution

Table 4 Electrochemical parameters of different materials in 1mol/L HCl solution

Samples	Self-corrosion potential, E_{corr}/mV	Self-corrosion current density, $i_{corr}/\mu A \cdot cm^{-2}$
45 steel	-497.00	379.31
Coating	-453.45	297.78

The corrosion properties of the cladding layer and the substrate in 3.5wt.% NaCl solution need to be further verified, and the impedance of the cladding layer and the electrochemical corrosion of the 45 steel matrix is fitted with the help of an equivalent circuit diagram, as shown in Fig. 8(a). Fig. 8(b) shows a Nyquist diagram of the coating and matrix in a 3.5wt.% NaCl solution. From Fig. 8(b), it can be seen that the coating and the 45 steel matrix form a single capacitive arc resistance, and the coating obtains a larger arc capacitive resistance than the substrate, indicating that the passivation film generated by the coating has better corrosion resistance, and the coating has better corrosion resistance than the matrix. The presence of the coating avoids direct contact between the matrix and the corrosive liquid, so that the matrix tissue is not corroded by the corrosive liquid. Fig.8(c) is the impedance modulus diagram of the cladding layer and the substrate, from which the impedance modulus of the cladding layer can be seen $|Z|$ impedance modulus greater than 45 steel matrix $|Z|$ further explains that the corrosion resistance of the cladding layer is better than that of the 45 steel matrix.

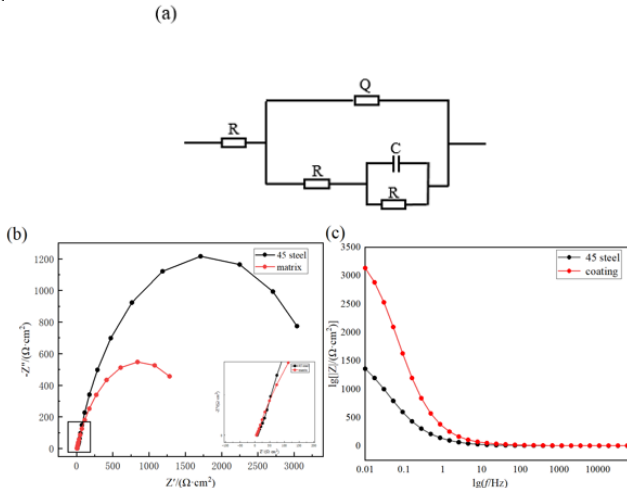


Fig. 8 Corrosion results of cladding layer and matrix in 3.5wt.% NaCl solution. (a) equivalent circuit; (b) Nyquist diagram; (c) impedance modulus diagram

Fig. 9(a) is an equivalent circuit for corrosion of the cladding layer and the matrix in a 1mol/L HCl solution. Fig. 9(b) is a Nyquist diagram of the cladding layer corroded with

the matrix in 1mol/L HCl solution. From Figure 9(b), it can be seen that the arc of the coating is greater than the arc of the steel matrix, indicating that the surface impedance of the substrate, and the corrosion resistance of the cladding layer is higher than the corrosion resistance of the matrix. In addition, the corrosion resistance of the material can also be expressed in the impedance modulus $|Z|$ on size. From fig. 9(c) impedance modulus diagram, it can be seen that the impedance modulus of the cladding layer is greater than the impedance modulus of the substrate, which further illustrates that the corrosion resistance of the coating is better than that of the 45 steel matrix.

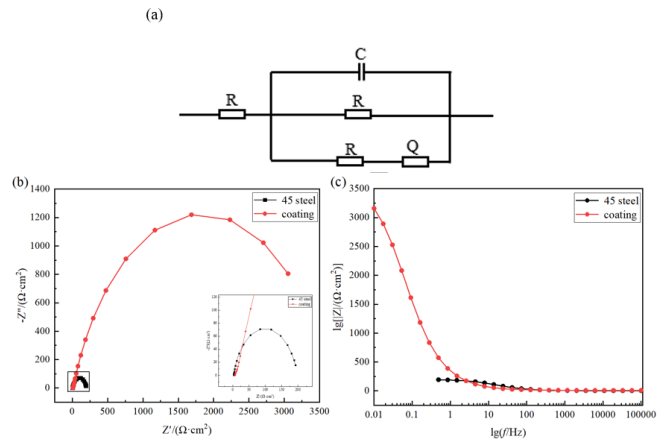


Fig. 9 Corrosion results of cladding layer and matrix in 1mol/L HCl solution. (a) equivalent circuit; (b) Nyquist diagram; (c) impedance modulus diagram

IV. CONCLUSION

- (1) Through uniform design experiments to explore the laser cladding process, combined with surface quality and dilution rate, the best process parameters are laser power 1050 W, scanning speed 10 mm/s, powder delivery capacity of 10 g/min, spot diameter of 2 mm, defocus amount of 13.8 mm, lap rate of 40%.
- (2) Laser cladding Fe-based alloy coating is densely microstructured, no cracks, porosity and other defects, the bottom of the coating is composed of dendrites thick branch crystals, the middle is composed of many grains that have lost their growth direction, and the top is mainly composed of isotonic crystals with small grains.
- (3) In NaCl solution, the self-corrosion potential of 304 stainless steel, Fe-based alloy coating and 45 steel matrix is reduced sequentially, the self-corrosion current is increased in turn, and the corrosion resistance is reduced in turn; the self-corrosion potential of Fe-based alloy coating, 304 stainless steel and 45 steel matrix in HCl solution is reduced sequentially, and the self-corrosion current is reduced from low to high as 304 stainless steel, Fe-based alloy coating, 45 steel matrix, and the corrosion resistance is reduced in turn.
- (4) By fitting the equivalent circuit, the arc-tolerant and capacitive-resist modulus of the cladding layer in NaCl solution and HCl solution are greater than the arc-capacitive resistance and the capacitive resistance modulus of the 45 steel matrix, so the corrosion resistance of the Fe-based alloy coating is significantly higher than that of 45 steel.

V. REFERENCES

[1] Yang X H, Chen J F, Wang Z, Chen G Y. Study on wear and corrosion resistance of Ni35 powder with laser claddi

- ng of steel surface[J].Thermal Processing Technology,2015,44(24):150-152.
- [2] Zheng C , Zhou Y . Surface modification of resistance welding electrodes by electro-spark deposited composite coatings: Part II. Metallurgical behavior during welding[J]. Surface & Coatings Technology, 2006, 201(6):2419-2430.
- [3] He Zhiyuan,He Wenxiong,YANG Haifeng. Research progress on laser cladding of aluminum alloy surface[J].China Surface Engineering,2021,34(06):33-44.
- [4] Zhang J Ch,Shi Sh H,GONG Yanqi,etc. Research Progress of Laser Cladding Technology[J].Surface Technology,2020,49(10):1-11.
- [5] Ding T,Zhang Y H,Li J J. Research status and prospect of laser cladding technology on stainless steel surface[J].Metal Heat Treatment,2022,47(02):205-212.
- [6] Fang Zh Zh, Qi W J, LI Zh Q.Effect of 304 Stainless Steel Laser Cladding Lap Rate on CoCrW Coating Microstructure, Wear Resistance and Corrosion Resistance[J].Materials Review,2021,35(12):12123-12129.
- [7] Liu Y . Microstructure and Corrosion Properties of Laser Cladding Fe-Based Alloy Coating on 27SiMn Steel Surface[J]. Coatings, 2021, 11.
- [8] Ricoa, Rodrigop, Mike Escalella Rodriguez. Korossien Resisteins Ben Al/West Clarsel Cladin Cotingsien a 6082 [Jay]. Collins, 2020, 10(7): 673.
- [9] Zhou J L, Kong Dejun. Corrosion wear and electrochemical corrosion behaviors of laser cladded amorphous FeSiB coating in 3.5% NaCl solution[J]. Materials Research Express, 2018, 6(3):35203-35203.
- [10] Wang Q, Yang J, Niu W, Li Y, Zhang K. Effect of La2O3 on Microstructure and Properties of Fe-based Alloy Coatings by Laser Cladding[J]. Optik - International Journal for Light and Electron Optics, 2021, 245(12):167653.
- [11] Zhu Y . Laser Cladding of Fe-based Alloy Coating on Axle Steel Surface[J]. Plating & Finishing, 2019.
- [12] Chen J F, Li X P, Xue Y P. Friction and Wear Properties of Laser Cladding Fe901 Alloy Coating on 45 Steel Surface [J]. Chinese Journal of Lasers, 2019, 46(5):0502001.
- [13] Qian S . Microstructure and Properties of Fe-based Alloy Coating by Laser Cladding[J]. Foundry Technology, 2019.